

N94- 35907

PLANAR ROTATIONAL MAGNETIC MICROMOTORS WITH INTEGRATED SHAFT ENCODER AND MAGNETIC ROTOR LEVITATION

H. Guckel, T.R. Christenson, K.J. Skrobis, J. Klein
Wisconsin Center for Applied Microelectronics
Department of Electrical and Computer Engineering
University of Wisconsin
Madison, WI 53706

55-33
11913
P-11

M. Karnowsky
Sandia National Laboratories
Albuquerque, NM 87185

ABSTRACT

Deep x-ray lithography and electroplating may be combined to form a fabrication tool for micromechanical devices with large structural heights, to 500 μm , and extreme edge acuities, less than 0.1 μm run-out per 100 μm of height. This process concept which originated in Germany as LIGA[1] may be further extended by adding surface micromachining[2]. This extension permits the fabrication of precision metal and plastic parts which may be assembled into three-dimensional micromechanical components and systems.

The processing tool may be used to fabricate devices from ferromagnetic material such as nickel and nickel-iron alloys. These materials when properly heat treated exhibit acceptable magnetic behavior for current to flux conversion and marginal behavior for permanent magnet applications.

The tool and materials have been tested via planar, magnetic, rotational micromotor fabrication. Three phase reluctance machines of the 6:4 configuration with 280 μm diameter rotors have been tested and analyzed[3,4]. Stable rotational speeds to 34,000 rpm with output torques above 10×10^{-9} N-m have been obtained. The behavior is monitored with integrated shaft encoders which are photodiodes which measure the rotor response. Magnetic levitation of the rotor via reluctance forces has been achieved and has reduced frictional torque losses to less than 1% of the available torque.

The results indicate that high speed limits of these actuators are related to torque ripple. Hysteresis motors with magnetic bearings are under consideration and will produce high speed rotational machines with excellent sensor application potential.

INTRODUCTION

In 1959 J.W. Beams reported on experiments in which he levitated a ferromagnetic sphere in a magnetic suspension in a hard vacuum environment[5]. The sphere with a diameter of a few hundred micrometers was rotated via magnetic induction to speeds above 50,000,000 rpm which eventually led to plastic deformation of the ferromagnetic material. The reported run-up and coast-down times were several days. Beams's experiment fundamentally contributed to gyro and ultra centrifuge progress. It is possible to argue that Beams's work also affects modern micromotor development in the sense that (a) his rotor diameter is of the same size as micromotor rotors and (b) that performance of micromotors which approaches Beams's results would have major implications on application possibilities for micromachines.

The challenges to micromotor fabrication and design in the present context are many. All micromotors will have small torque outputs. This is simply a consequence of available energy density and working volume. Since maximum energy densities for magnetics and electrostatics are fixed and the working volume is small the low torque output statement is justified. The argument can be taken one step further: micromachines with a small chip area profit from construction techniques which utilize the structural height of the device for volume and therefore torque increases.

With small output torques motor losses must be minimized. In the present context this implies a non-contact bearing and, of course, hard vacuum operation. Since true electrostatic and magnetic bearings are open circuit unstable appropriate sensors and feedback mechanisms become part of the motor design.

The third point involves the motor type. Micromotors have a small moment of inertia. This is good and bad. If the torque versus rotational angle behavior of the machine has large ripple the machine will become a stepping motor which will cause major problems with maximum speeds because the rotational speed will become angle dependent and pole

overshoot will lead to synchronization problems[6]. A constant torque versus rotational angle behavior avoids this issue and simplifies motor control schemes significantly.

The driving mechanism for the anticipated machine can be electrostatic or magnetic. Maximum energy densities are slightly larger for magnetics. Processing convenience favors electrostatics because the structures are less three dimensional than magnetic devices because of the enveloping coil requirement for current to flux conversion. The motor control aspect for rotational speed to 1×10^6 rps and possibly many pole configurations require microelectronics with fairly high clock rates. Integrated circuits for high speed current switching, and magnetics are available. High speed, high voltage control circuitry is much more limited. System perspectives do therefore favor magnetics for the immediate future. The torque ripple issue which is a severe problem for nearly all electrostatic machines tilts the implementation towards magnetics.

MAGNETIC MOTOR FABRICATION AND DESIGN

In the previous section the goals for a high speed motor program have been discussed. The stated requirements are of course very ambitious and are subdivided into a preliminary phase with the goals of (1) providing a planar magnetic motor (2) demonstrating a one-dimensional magnetic bearing and (3) incorporating rotor position sensors.

The technology of choice is a combination of integrated circuit processing, deep x-ray lithography and metal plating and surface micromachining. The motor design is that of a three phase machine: six poles, with a salient rotor with symmetry about the x and y axis. Levitation is provided by fabricating the rotor at a structural height which is less than the stator height and therefore produces an upward force due to the stator field. The rotor support shaft is fluted to reduce frictional losses and to produce centering via currents during atmospheric operation. Rotor position sensing is achieved by a shaft encoder which is formed from diffused photodiodes which are located in the substrate. Figure (1) illustrates the general concepts.

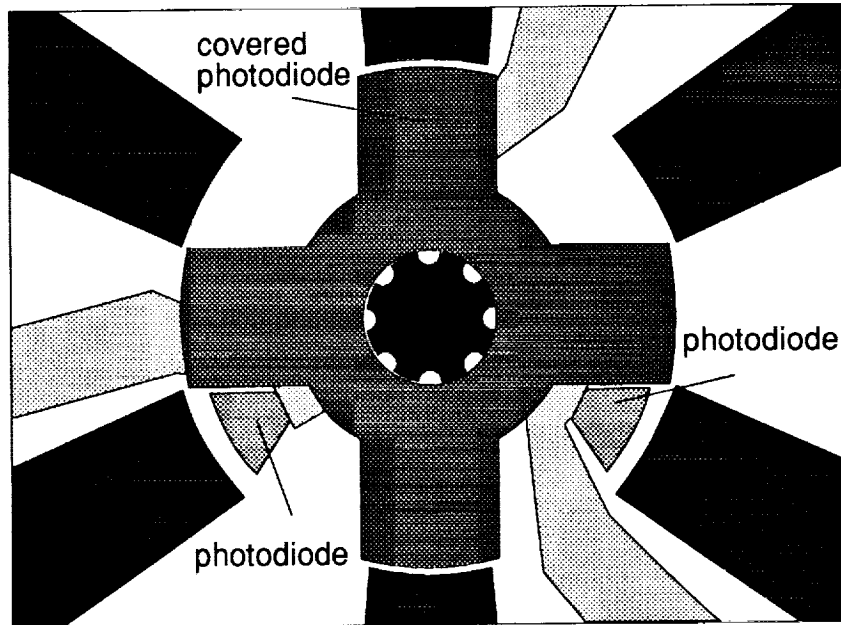


Figure 1. Stator, rotor, fluted shaft and photodiode layout.

The processing sequence starts with a 3" silicon substrate which is oxidized and patterned with the photodiode diffusion mask via standard IC-processing. The passivated substrate is next covered with a nickel layer which is patterned with the lower sections of the coil windings which will eventually surround the magnetic material. These coils will have to be insulated which implies a dielectric cover which in the present case is formed by a layer of chemical vapor deposited oxide. Both of these processes, nickel and oxide deposition, are more or less standard integrated circuit processing procedures; the same comment applies to the removal of the oxide over the nickel in the area in which the vertical sections of the coil are to be attached.

The procedures become unusual in the next sequence which deals with surface micromachining. A sacrificial layer of soft polyimide is applied and patterned in those areas of the wafer in which for instance free magnetic structures such as the rotor are to be produced. After this process the entire wafer is covered with a sputtered plating base: 150Å of titanium followed by 150Å of nickel. These procedures are again nearly routine IC-fabrication procedures.

Unusual processing which is related to the high structural height requirement starts at this point. The wafer is covered with a casted film of x-ray sensitive photoresist. The thickness of this layer is typically 300 micrometer which is of course very unusual for

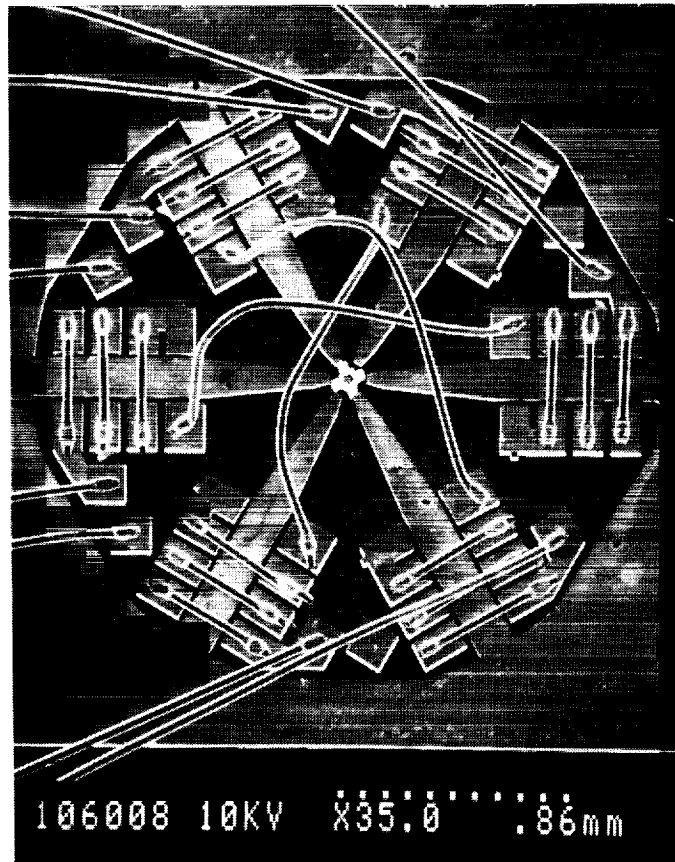


Figure 2. SEM photograph of completed integrated planar magnetic micromotor. The configuration is that of a 6 pole stator and 4 pole rotor stepping motor with six turns per pole pair.

photoresist thicknesses which are typically near 1 micrometer. The x-ray photoresist is exposed by using synchrotron radiation with wavelengths between 2 to 3 Å, through an x-ray mask which is aligned to the working substrate. Because synchrotron radiation is collimated very well and x-ray absorption cannot produce standing waves, developing of the exposed pattern produces a photoresist mold with nearly perfect definition and, in particular, pattern run-out of less than 0.1 μm per 100 μm of structural height. The developed mold recesses are next filled with electroplated metal: in the present case nickel or permalloy 80% Ni, 20% Fe. The x-ray photoresist is removed, any unwanted plating base is etched off and the sacrificial layer is chemically dissolved. The substrate now consists of fully attached parts such as the stator with partially finished coils and the center hub and of course free parts such as the rotor. The coils are completed by wire bonding with 30 μm diameter wire. The rotor is assembled to the shaft in a micromanipulator and the device as shown in Fig. 2 is ready for testing.

The actual design of a planar micromotor insists on closed magnetic circuits which are in the plane of the substrate. The total reluctance in this geometry involves not only the two air gaps between rotor and stator but also the reluctance of the rotor and the flux return path. Since the return path reluctance is parasitic on motor performance it must be minimized to obtain maximum gap flux. This minimization involves the magnetic properties of the material: a high permeability is desirable and the geometry: short path lengths with large cross-sections are favored. In this sense, the chip area which a motor for given torque output uses becomes very much a function of magnetic material properties.

The processing tool as discussed here can produce shaft to rotor clearances which are submicron. The reason for this is found in the fact that assembly implies shaft to rotor clearances which are obtained by subtracting two optically defined dimensions. These two individual dimensions cannot be submicron. However, their differences can. This observation together with the low flank run-out allows the fabrication of motor air gaps with demonstrated dimensions of less than $0.25 \mu\text{m}$. This is advantageous from two perspectives: reduced friction due to precision bushings and large potential magnetic gap pressures. These large magnetic flux densities can, however, only be achieved if the return path reluctance is small in comparison to the gap reluctance. This condition has not been achieved with pure annealed nickel ferromagnetics. However, recent improvements in magnetic materials as shown in Figure 3 allow designs with magnetic flux densities in the gap of better than 3000 gauss.

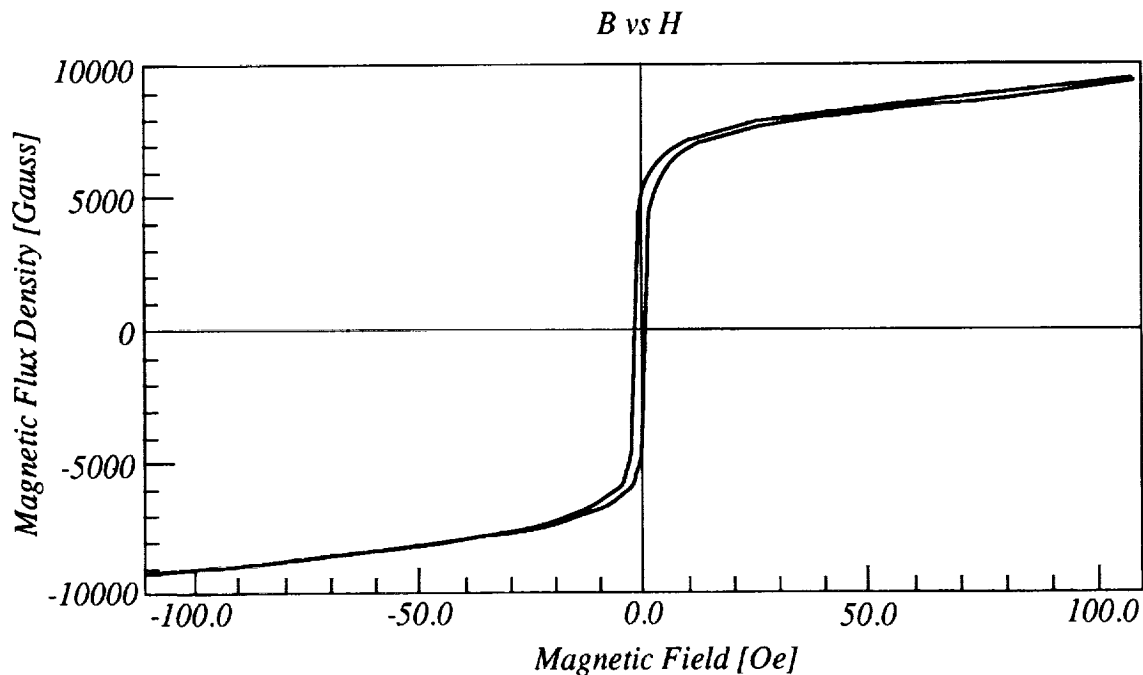


Figure 3. Magnetic behavior of as deposited ^{78}Ni - ^{22}Fe permalloy.

In the current motor designs rotor thickness is less than stator thickness. This implies that the rotor will levitate in the stator field. The amount of levitation depends on the gap flux and the weight of the rotor. Self-centering can be achieved if the motor shaft is fluted and if the device is operated in modest pressure ambients. Theoretical analysis of the detailed rotor behavior requires at the very least a three-dimensional magnetic field analysis which can also estimate the motor torque output. This has been achieved by using Flux 3D[7]. The anticipated results are shown in Fig. 4.

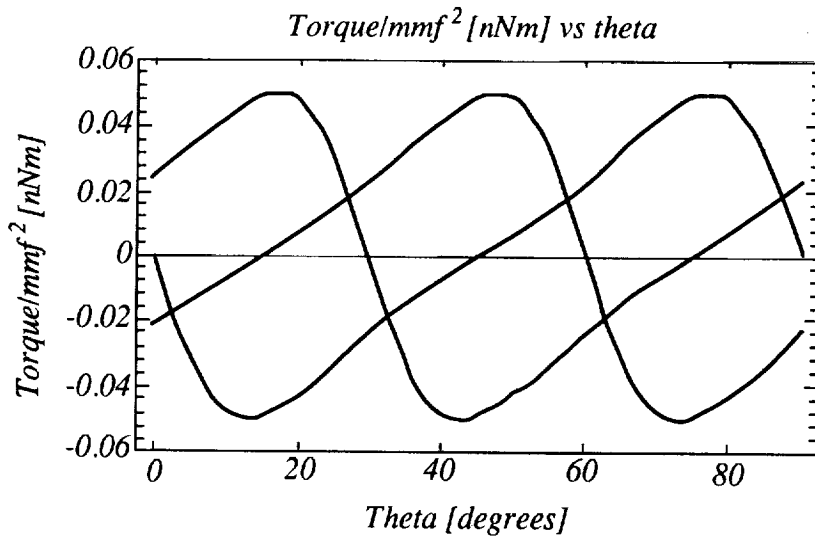


Figure 4. Simulated normalized torque curves for 90° of motor rotation. Stator-rotor alignment occurs at 0° and every 30° thereafter. These curves assume a square wave excitation. The current excitation waveform shape will modulate these torque curve shapes further. These curves apply to a motor which has a $285\ \mu\text{m}$ diameter rotor, $80\ \mu\text{m}$ in thickness centered about a stator of $160\ \mu\text{m}$ thickness.

Software which can handle fluid mechanics and magnetics or mechanical deformation due to magnetic forces is not available. It would aid design tremendously.

TEST RESULTS

In order to test experimental structures the motors are packaged into flat packs as shown in Figure 5.

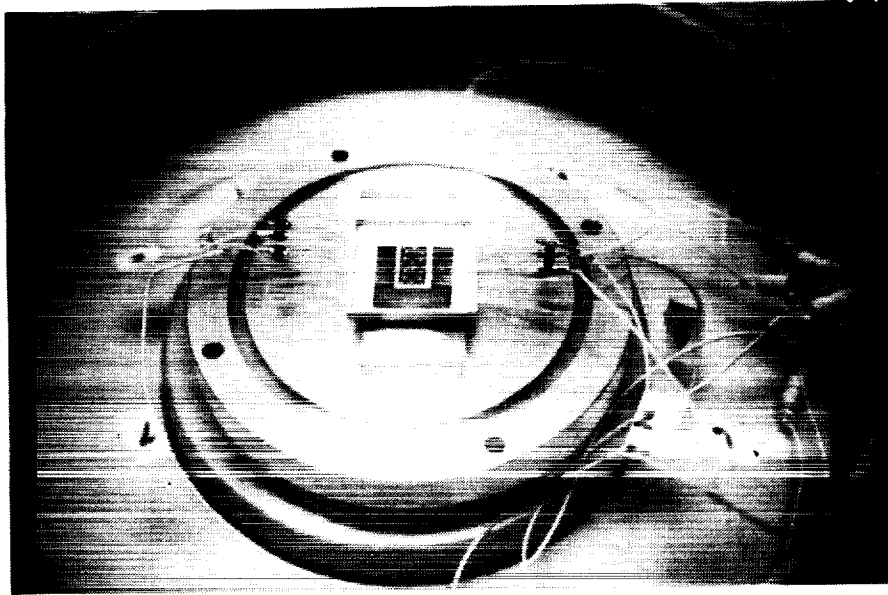


Figure 5. Packaged micromotor shown in vacuum system.

Motor behavior is studied via visual examination which typically involves video tapes. Much more detailed data is obtained from the photodiode shaft encoder. Both data sets result in the conclusion that this type of reluctance motor functions as a stepping motor with significant pole overshoot. This overshoot causes a loss of synchronization for open loop operation and therefore a maximum open loop rotational speed. The estimated failure frequency is given by

$$f_N = \frac{1}{2\pi} \left(\frac{T'}{J_R} \right)^{\frac{1}{2}} \quad (1)$$

Where T is the slope of the torque curve near rotor alignment and J_R the rotor polar moment of inertia[8,9]. Typical values for a 280 μm rotor which is 80 μm thick and is suspended in a 160 μm tall stator are $J_R = 1.7 \times 10^{-16} \text{ kg} \cdot \text{m}^2$ if the shaft diameter is 72 μm with a torque slope of ... The predicted maximum rotational speed becomes 44,000 rpm. Experimental data resulted in a maximum speed of 33,000 rpm. A word of caution is in order: these speeds refer to open loop operation with non-overlapping square wave excitation on the three phases. For these test conditions which were performed in room air ambients frictional losses are roughly 0.5% of available torque. A comparison of room

ambient to vacuum operation did not change the upper speed significantly and produced no significant modification in the pole overshoot behavior. The frictional loss appears to come from shaft friction which is low because of shaft geometry and the inherently low radial forces for this type of machine. A new design with improved magnetic material and smaller rotor radius has been constructed. It is anticipated that rotational speeds above 100,000 rpm will be achieved.

Rotor levitation during these tests is roughly 45 μm . Substrate friction is therefore absent. Long term testing at maximum speed did not affect motor performance. Shaft wear via electron microscope examination was not detectable.

CONCLUSIONS

Planar reluctance motor design, construction and testing have been accomplished in the presence of a one-dimensional magnetic bearing and integrated shaft encoder. Experimental and theoretical performance are in rough agreement.

The use of micromotors for very high speed operation hinges on two issues: torque ripple and friction. Torque ripple is inherent to reluctance motors which are expected to peak out between 100,000 and 200,000 rpm. This class of motors will therefore not achieve very high speed directly but could do this by step-up gear boxes and closed loop control. Other motor types, for instance hysteresis motors, have inherently less torque ripple and are currently under investigation[10].

Frictional losses must be reduced significantly for high speed devices. This can be accomplished by two methods: a true magnetic bearing for which the position sensors have already been demonstrated or a form of non-contact bearing which is unique to micromechanics. Both approaches are under active investigation.

The available torque output from micromotors, currently 20×10^{-9} Newton - meter, can be improved significantly. If this torque is available with minimized ripple and non-contact bearings, micromotors will approach Beams's experimental results. Ramp speeds which in Beams's case involved several days to reach maximum speed will be comparable and acceptable even if modest angular momentum storage devices are to be driven by this type of machine.

ACKNOWLEDGMENTS

This work was supported in part by the National Science Foundation under grant ECS-9116566. The contribution of Mr. Dale T. McGuffin (Sandia Laboratories) with metallography support is gratefully acknowledged. Mr. T. Martin's (Quantum Devices Inc.) assistance with wire bonding is greatly appreciated. We acknowledge the support of the staffs of the Center for X-ray Lithography and the Synchrotron Radiation Center for their help and the use of their facilities. The Center for X-ray Lithography is supported by SEMATECH Center of Excellence SRC Grant No. 88-MC-507 and the Department of Defense Naval Research Laboratory Grant No. N00014-91-J-1876. The Synchrotron Radiation Center is supported by the National Science Foundation, grant DMR-88-21625.

REFERENCES

- [1] E.W. Becker, W. Ehrfeld, P. Hagemann, A. Maner, D. Münchmeyer, "Fabrication of Microstructures with High Aspect Ratios and Great Structural Heights by Synchrotron Radiation Lithography, Galvanofarming, and Plastic Moulding (LIGA Process)," *Microelectronic Engineering*, 4, 1986, pp. 35-56.
- [2] H. Guckel, T. Christenson, and K. Skrobis, "Metal Micromechanisms via Deep X-Ray Lithography, Electroplating, and Assembly," Proceedings of Actuator '92, Bremen, Germany, June 1992, pp. 9-12.
- [3] H. Guckel, T.R. Christenson, K.J. Skrobis, T.S. Jung, J. Klein, K.V. Hartojo, and I. Widjaja, "A First Functional Current Excited Planar Rotational Magnetic Micromotor," Proceedings of IEEE Micro Electro Mechanical Systems (MEMS '93), Fort Lauderdale, FL, USA, Feb. 1993, pp. 7-11.
- [4] H. Guckel, T.R. Christenson, K.J. Skrobis, J. Klein, and M. Karnowsky, "Design and Testing of Planar Magnetic Micromotors Fabricated by Deep X-Ray Lithography and Electroplating," in Digest of Technical Papers, 7th International Conference on Solid-State Sensors and Actuators-Transducers '93, Yokohama, Japan, 7-10 June 1993, pp. 76-79.
- [5] J.W. Beams, "High-Speed Rotation," *Physics Today*, July 1959, pp. 20-27.
- [6] C.K. Taft, R.G. Ganthier, T.J. Harned, *Stepping Motor System Design and Analysis*, University of New Hampshire, 1985.

- [7] Magsoft Corporation, FLUX3D, Troy, New York.
- [8] Y.C. Tai and R.S. Muller, "IC-Processed Electrostatic Synchronous Micromotors," *Sensors and Actuators*, 20, 1989, pp. 49-55.
- [9] J. Cernus and V. Hamata, *Transient Stability Analysis of Synchronous Motors*, New York: Elsevier, 1990.
- [10] B.R. Teare, Jr., "Theory of Hysteresis - Motor Torque," *AIEE Transactions*, Vol.59, 1940, pp. 907-912.

